IJE TRANSACTIONS A: Basics Vol. 38 No. 10, (October 2025) 2394-2404

International Journal of Engineering

Journal Homepage: www.ije.ir

Modelling of Highway Traffic Using a Triangular Fundamental Diagram with Hybrid Petri Net Continue

H. Luthfiyah*[a], A. S. Yunata[b], M. S. Harjono[a], A. Halim[c]

[a] *Research Center for Transportation Technology, National Research and Innovation Agency, Serpong, Indonesia*
[b] *Research Center for Electronics, National Research and Innovation Agency, Serpong, Indonesia*
[c] *Department of Electrical Engineering, Faculty of Engineering, Universitas Indonesia, Depok, Indonesia*

PAPER INFO

Paper history:
Received 30 September 2024
Received in revised form 15 January 2025
Accepted 24 January 2025

Keywords:
Macroscopic Model
Highway Traffic
Triangular Fundamental Diagram
Hybrid Petri Net Continue
Simulation Analysis

ABSTRACT

This paper focuses on creating a macroscopic traffic flow model that describes crucial traffic dynamics: density, traffic flow, and average speed. Changes in traffic flow dynamics are captured through a simplified macroscopic traffic flow model with a triangular shape, which allows the system to respond quickly to developments in real-world conditions. The triangular shape model is called the Triangular Fundamental Diagram (TFD), which represent substantial traffic condition namely free-flow, equilibrium flow, and congested flow conditions. This research employs Hybrid Petri Net (HPN) Continue and the SimHPN simulator to develop the TFD model. Subsequently, the TFD-HPN Continue model is applied to a case study involving traffic on the Pasteur highway. The paper successfully introduces a macroscopic traffic flow model, TFD, and pairs it with the HPN Continue approach to simulation. The simulation results showed that the differences between the TFD-HPN Continue model and the MFD model are as follows: K_{crit} by 1.87%, q_{max} by 0.74%, and K_{jam} by 0.12%. In summary, the TFD-HPN Continue model demonstrates its ability to resemble real-world traffic dynamics through its application to the Pasteur highway case.

***doi**: 10.5829/ije.2025.38.10a.15*

Graphical Abstract

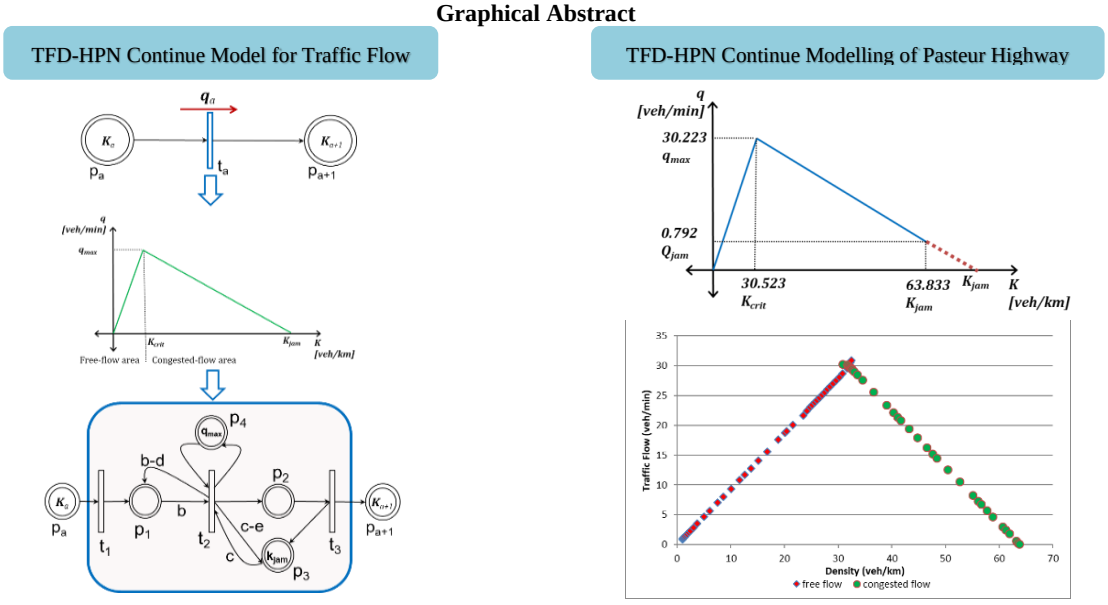

*Corresponding Author Email: hilda.luthfiyah@brin.go.id (H. Luthfiyah)

Please cite this article as: Luthfiyah H, Yunata AS, Harjono MS, Halim A. Modelling of Highway Traffic Using a Triangular Fundamental Diagram with Hybrid Petri Net Continue. International Journal of Engineering, Transactions A: Basics. 2025;38(10):2394-404.

NOMENCLATURE

q_i	traffic flow of large vehicles (veh/km)	P	set of vertices *place p*, $\boldsymbol{P} = \{p_1, p_2, p_3, \ldots, p_n\}$, with $n \geq 0$
K	number of vehicles within a specific road section (veh)	T	set of nodes *transition t*, $\boldsymbol{T} = \{t_1, t_2, t_3, \ldots, t_m\}$, with $m \geq 0$
$V_{e,HFD}$	average vehicle speed on road section *i* (km/h)	***Pre***	input or pre-incident matrix that contains the set of weights for each arrow (*arc*) from a *p* to *t*, *mapping the input* $\boldsymbol{P} \times \boldsymbol{T} \rightarrow \{0,1\}$
V_{free}	average vehicle speed obtained from actual field measurements under free-flow conditions (km/h)	**Post**	set of weights for each weight (*arc)* from *t* to a node *p* (it is also called the output matrix, as it represents the arrow weights after the *transition* process, *mapping output* $\boldsymbol{P} \times \boldsymbol{T} \rightarrow \{0,1\}$),
K_{crit}	number of vehicles at the critical point on road section *i* (veh/km)	m_0	set of initial token values of the network *p* before *firing* occurs
i_{HFD}	correction coefficient applied to the results of actual field measurements for stationary mean velocities in MFD	α	*firing* value for a single *firing*, within the range $0 < \alpha < enab(t_j, m)$
K_{jam}	vehicle density at which traffic becomes saturated or highly congested (veh/km)	$C(\cdot, t_j)$	network notation for one-time *firing*, where the *C* matrix corresponds to a single t_j with a set *place* at the time of $\boldsymbol{Pre} \cdot t_j$.
q_{max}	maximum traffic flow (veh/km)	m	set of token matrices in *p* after *firing*
C	matrix representing the dynamics of the overall flow of token evolution	σ	firing counter vector with a value greater than or equal to zero
f	flow of the *transition*		

1. INTRODUCTION

Efficient monitoring and traffic management on highway networks remain a challenge for researchers and traffic practitioners, especially in urban areas. Highways are designed to be free from obstructions caused by vehicles with less than four wheels. However, congestion on highways is now common, particularly during peak times, due to the increasing number of vehicles. Congestion can also result in from accidents. Using Machine Learning (ML), recent research has successfully modeled the factors contributing to accidents and predicted the likelihood of future occurrences (1-3). Traffic management on highways aims to regulate vehicle density, ensuring a smooth flow of traffic and preventing severe congestion. Traffic management involves creating traffic models to design, predict, and control traffic systems (4). This process includes modeling traffic flow dynamics for each element in a highway network, which is complex due to the large number of entry and exit points, and highway gate. One method for simulating these dynamics is the use of macroscopic traffic models, which utilize aggregate quantities to represent traffic flow, making calibration easier. Traffic aggregates are analogous in hydrodynamics principles, with dynamics described by variables such as flow, density, and average speed. Macroscopic traffic simulation models assist policymakers in making more informed decisions, leading to more efficient movement of people and goods, enhanced safety, and reduced environmental impacts (5).

Traffic flow consists of a heterogeneous system with two types of behavior: continuous and discrete (6). Continuous traffic flow is uninterrupted and results in from the interaction between vehicles within the traffic stream and the characteristics of the road (geometric and environmental). Discrete flow occurs at access points that can periodically stop or significantly slow down traffic. For example, in macroscopic traffic models based on divided space and time variables, continuous flow occurs on highways, while discrete flow occurs at highway segments with entry/exit points (7). The advantage of macroscopic traffic models is their flexibility and speed in system calibration, as well as being more computationally efficient compared to microscopic models (8).

Macroscopic traffic models are depicted as fluid flow, with both continuous and discrete forms. Petri Net (PN) is a tool that can be used to model traffic networks by representing both continuous and discrete system events. The application of PN in continuous traffic modeling can be seen on freeways using Continuous Timed Petri Nets (CTPN) (9, 10). For discrete events in PN, examples include signalized intersections (11), Traffic Light Control (TLC) using Hybrid Petri Net (HPN) (12), and TLC using Timed Petri Net (TPN) (13). PN applications also extend to urban road networks, such as those using Colored Petri Nets (CPNs) (14) and using Probabilistic Petri Nets (PPN) (15). On a microscopic scale, PN is used for PN-based sequence modeling to address collision avoidance system challenges and to improve the behavior of Connected and Autonomous Vehicles (CAV) (16).

The simplest and most commonly used first-order macroscopic traffic flow model is the Cell Transmission Model (CTM), the model obtained by dividing one road section into several cell segments (17). All joined cells have the same length, path, radius, and curvature (homogeneous). CTM is represented through Triangular Fundamental Diagram (TFD) to illustrate the relationship between density and flow (18). TFD is a simplified version of the Macroscopic Fundamental Diagram (MFD), which describes the aggregate number of vehicles entering a road segment and the completion flow, defined as the output flow of that segment. The

MFD is easier to calibrate and is more suitable for real-time applications or when involving larger traffic networks (4). In the TFD, network flow increases with density accumulation up to a critical point, after which additional vehicles in the network cause a significant reduction in flow as completion flow. The TFD simplifies the control of vehicles entering road segments or highways.

HPN are a formal method for modeling systems involving both discrete and continuous events. They offer graphical capabilities for constructing modular models and support algebraic mathematical formulation in matrix form, making HPN suitable for modeling macroscopic vehicle flows with discrete events, such as traffic flow at toll gates. This approach differs from the Cellular Automaton (CA) model, which is a stochastic, discrete automaton model developed to simulate freeway traffic, represented as a one-dimensional array in discrete form. In contrast, agent-based models are more appropriate for microscopic traffic flow simulations.

Based on previous research, TFD modeling using HPN Continue has not yet been conducted. Therefore, this study aims to develop a new approach model, specifically a TFD for a single road segment using HPN Continue, where each road segment assumption has a uniform macroscopic model. The TFD was chosen because it can quickly respond to changes in traffic conditions, as traffic flow data is dynamic. The advantage of using HPN Continue is its ability to represent traffic stochastically. This TFD model is tested using data from the highway network in Bandung to evaluate the effectiveness of the TFD-HPN Continue. The simulation is carried out with the HPN Simulator (SimHPN) to depict various traffic scenarios, such as free flow, equilibrium state, and congested conditions (19). The paper is structured as follows: Section 2 outlines overview traffic model; Section 3 introduces the Hybrid Petri Net Continue and TFD-HPN Model; Section 4 explains data retrieval; Section 5 presents the results and discussion, followed by the conclusion.

2. OVERVIEW TRAFFIC MODEL

2. 1. Macroscopic Traffic Model The macroscopic traffic model is created by discretizing a road segment, using the average vehicle movement over a specific period (20). The number of vehicles in a certain road area is calculated by measuring the difference between the incoming and outgoing traffic flow over a set time interval. From these variables, a macroscopic traffic model is developed, linking vehicle density and traffic flow (21). The fundamental diagram of the macroscopic traffic model must represent all traffic conditions on the road segment within a specific time scale, ensuring that each model parameter reaches a stable point. Ultimately, the properties of the fundamental traffic diagram, known as MFD, should achieve equilibrium. The MFD parameters for road section i described the dynamics of the influence of traffic flow q_i on vehicle density K under equilibrium conditions, based on the hydrodynamic principle (22) can be seen in Figure 1.

The equation for calculating the average vehicle speed using the hydrodynamic principle is provided in Equation 1.

$$V_{e,HFD}(K) = V_{free} \cdot \exp\left[-\left({}^{1}/_{i_{HFD}}\right)\cdot\left({}^{K}/_{K_{crit}}\right)^{i_{HFD}}\right] \quad (1)$$

The traffic flow rate of vehicles passing through road section i, qi for ρ(K) = K can be defined based on Equation 2.

$$q_i = K \cdot V_{free} \cdot \exp\left[-\left({}^{1}/_{i_{HFD}}\right)\cdot\left({}^{K}/_{K_{crit}}\right)^{i_{HFD}}\right] \quad (2)$$

2. 2. TFD Model The equation for the fundamental diagram of equilibrium, with parameters for vehicle flow and density, was mathematically simplified by Daganzo (23) into a triangular form known as the TFD. The simplification of MFD to TFD allows for a quicker response to the dynamics of the macroscopic traffic model without compromising measurement accuracy (24, 25). This simplification is based on the relationship between incoming traffic flow (*demand* Δe) and available road space (*supply* $\sum e$), resulting in a traffic flow function q that depends on vehicle density K. Figure 2 illustrates how changes in the number of vehicles entering and exiting a road section affect the traffic flow $q_{xa}(t)$. The road network is divided into sections, with each section assumed to be homogeneous and exhibit TFD characteristics. Each road section of length l_a begins at point x_a where vehicles enter, and extends to point x_{a+1}

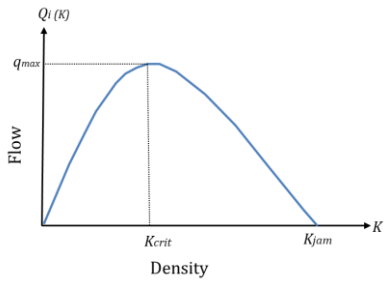

Figure 1. Vehicle Speed, density, and Flow Relationships

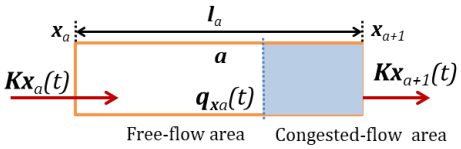

Figure 2. Traffic flow on a single road section scheme

where vehicles exit. During the time interval t to $t+\Delta t$, K vehicles enter the road section, defined as $Kx_a(t)$, while $Kx_{a+1}(t)$ vehicles exit the section.

Figure 3 shows the relationship between *demand* Δe and *supply* $\sum e$, which creates a TFD. If a road section has a length l_a and the variables *demand* Δe and *supply* $\sum e$, the traffic flow dynamics qx_a can be plotted against the number of vehicles K over time. K_{crit} represents the vehicle density at which maximum traffic flow q_{max} occurs. K_{jam} indicates the vehicle density at which traffic becomes saturated or highly congested, causing the flow to approach zero or come to a complete stop. Figure 3 illustrates vehicular traffic flow $q_a(K)$ divided into two phases. The first phase is the free flow condition, occurring when the number of vehicles is within the range $0 < K < K_{crit}$, with the average speed denoted as V_{free}. The second phase represents the congested flow, occurring when the number of vehicles falls within $K_{crit} < K < K_{jam}$ with the average speed labeled V_{wave}. The transition from free flow to congested flow occurs through an equilibrium flow, where the number of vehicles K equals K_{crit} and the vehicle traffic flow reaches the maximum value $q_{max,a}$ for that road section.

Equation 3 models the potential arrival traffic flow *demand* $\Delta e(K)$ on road section a as shown in Figure 3.

$$\Delta_{e,a}(K) = \begin{cases} q^d_{e,a}\big(\rho(K)\big), \text{for } K \le K_{crit} \\ q_{max,a}\,, \text{for } K_{crit} < K < K_{jam} \end{cases} \quad (3)$$

For road section i, if the number of vehicles K is less than or equal to the critical number of vehicles K_{crit} then the demand equation $\Delta_e(K)$ is represented by $q^d_{e,a}\big(\rho(K)\big)$. This equation is a linear function of traffic flow potential along a line connecting the points (0,0) and (K_{crit}, q_{max}). However, if the number of vehicles on road section i falls between K_{crit} and K_{jam} (when the vehicle density reaches saturation), the traffic flow equals $q_{max,a}$.

The mathematical equation that represents the available road space, or supply $\sum_{e,a}(K)$ for a single road section a is shown in Equation 4.

$$\sum_{e,a}(K) = \begin{cases} q_{max,a}\,, \text{for } K \le K_{crit} \\ q^s_{e,a}\big(\rho(K)\big), \text{for } K_{crit} < K < K_{jam} \end{cases} \quad (4)$$

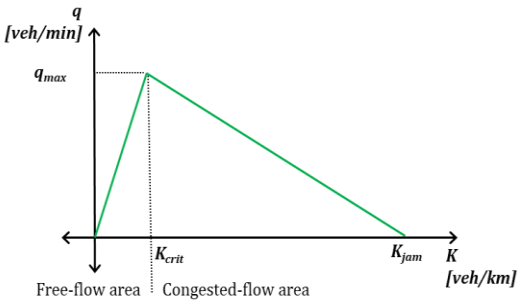

Figure 3. TFD model

If the number of vehicles K is less than or equal to K_{crit}, the traffic flow reaches its maximum, $q_{max,a}$, on road sections a. When K exceeds K_{crit} but remains below the saturation level K_{jam}, the road space availability, or supply $\sum_{e,a}(K)$, is modeled by $q^s_{e,a}\big(\rho(K)\big)$, which is a linear function approaching traffic flow at saturation. This function forms a line from (K_{crit}, q_{max}) to (K_{jam}, 0).

The resulting traffic flow q as a function of density $\rho(K)$ is given by Equation 5, which uses the minimum function operator **min**. This operator selects the smallest value between *demand* Δe and *supply* $\sum e$, effectively synchronizing traffic flow.

$$q_a(K) = \mathbf{min}\,[\Delta_{e,a}(K), \sum_{e,a}(K)] \quad (5)$$

3. HPN CONTINUE

HPN is a models of discrete event systems with analysis and simulation methods based on discrete and continuous Petri nets simultaneously in one structure (26, 27). The $\mathcal{N}$ network structure in HPN modeling consists of five components, namely:

$$\mathcal{N} = \langle P, T, Pre, Post, m_0 \rangle \quad (6)$$

Each *arc* has only one direction. The weights for an *arc* in the **Pre** and **Post** matrices are represented as $\boldsymbol{Pre}, \boldsymbol{Post} \in \mathbb{R}_{0+}^{|P|x|T|}$. For the initial token values in the set m_0 the weights are represented as $\boldsymbol{m_0} \in \mathbb{R}_{0+}^{P}$. These weights are non-negative real numbers and do not have to be integers.

The HPN model consists of both discrete and continuous node components simultaneously. Specifically, the system is piecewise linear, with *transitions* governed by the *minimum-operator* principle. This principle applies to both the **Pre** and **Post** matrices, representing the states before and after *events*, respectively. The token flow matrix is determined by the difference between the **Post** and **Pre** matrices, symbolized as matrix-vector C on Equation 7.

$$C = Post - Pre \quad (7)$$

3. 1. HPN Continue Execution A change in the token's value at a place occurs due to a *transition*. The flow of token movement can vary dynamically, a process known as token evolution (marking evolution). This *event* begins with the activation (enabling) of a *transition* (27, 28). The enabling of t occurs if the number of tokens m_a from p_a is at least equal to the *weight* of the incident **Pre** matrix, which maps the relationship from p to t_j. According, the rule states that all *places* connected to a continuous *transition* will be considered to have continuous tokens, even if their initial marking value is $\boldsymbol{m_0} \in \mathbb{N}_{\geq 0}^{|P|}$. The activation process differs for discrete

transitions T^d and continuous *transitions* T^c, as described in Equation 8. In T^d, the enabling degree is calculated using the minimum operator (**min** symbol) and rounding down (⌊ ⌋) to the nearest natural number and greater than zero or $\boldsymbol{enab}(t_j,\boldsymbol{m})\in\mathbb{N}_{>0}$. In a T^c, the synchronization process aims to obtain an enabling degree value that satisfies $\boldsymbol{enab}(t_j,\boldsymbol{m})\in\mathbb{R}_{>0}$.

$$enab(t_j,m)=\begin{cases} min_{p_a\in t_j}\left\lfloor\frac{m_a}{Pre(p_a,t_j)}\right\rfloor, \text{if } t_j\in T^d \\ min_{p_a\in t_j}\frac{m_a}{Pre(p_a,t_j)}, \text{if } t_j\in T^c \end{cases} \quad (8)$$

If the enabled state is maintained at a *transition*, the *transition* is ready to perform token release (*firing*). *Firing* is the process of moving tokens, enabled by the *transition*, with specific weights from *t* to *p* in the **Post** matrix. The *firing event* at *t* leads to token evolution (marking evolution). The increase in token count *m'* after a single *firing* is the result of the change in the number of tokens before *firing m*, as defined in Equation 9.

$$m'=m+\alpha\cdot C(\cdot,t_j) \quad (9)$$

Multiple sequential *firing* events will result in a new token value, each one evolving from the previous *firing*. The new token value at the end of the *firing* process is described by Equation 10, known as the fundamental equation.

$$m=m_0+C\cdot\sigma \quad (10)$$

Firing on continuous *transition* T^C influenced by the time function, Equation 11 becomes:

$$m(\tau)=m_0+C\cdot\sigma(\tau) \quad (11)$$

The *firing* vector $\sigma(\tau)$ is influenced by the time function over the interval [0, τ]. The flow of tokens is derived from the derivative of Equation 12, which then produces the derivative of the token evolution resulting from the firing.

$$\dot{m}=C\cdot f \quad (12)$$

3. 2. Infinite Server Semantic The infinite server semantic model defines how an *event* is executed (*firing*) in *t*. The amount of token flow ft_a is influenced by the mean speed of internal firing in *transation* λ_{ta} and a specific minimum threshold value required to appropriately activate the transition appropriately (28). Thus, the equation for ft_a is given in Equation 13.

$$f_{t_a}=q_a=\lambda_{t_a}\cdot enab(t_a,m_a)=\lambda_{t_a}\cdot min_{p_a\in t_a}\left\lfloor\frac{m_a}{Pre(p_a,t_a)}\right\rfloor \quad (13)$$

3. 3. HPN Continue Modeling of TFD Model Our study adopts TFD for HPN Continue modeling to create a more representative model that allows for a quicker response to traffic flow dynamics. The firing class used in this transition decomposition is a *timed continuous transition* with *infinite server semantics firing*. The evolution of this model is governed by the fundamental diagram (Equation 4). As shown in the top part of Figure 4, the base model of HPN Continue consists of each road section *a* exhibits traffic flow dynamics represented by q_a, which are stored on t_a. The number of vehicles entering the road section *a*, denoted as K_a, is represented by the tokens stored in p_a. Meanwhile, the dynamics of the traffic flow result in vehicles exiting the road section $a+1$, denoted as K_{a+1}, which are stored in p_{a+1} .

To model the dynamics of vehicles entering and exiting road sections, including free flow, steady-state flow, and congested flow, the HPN Continue model simulates these conditions through the decomposition of t_a. t_a is further detailed using the TFD model from Figure 3 and then transformed into the HPN Continue model. The TFD-HPN Continue model consists of: 3 *transitions* $,T=\{t_1,t_2,t_3\}$; 6 places, $P=\{P_i, P_1, P_2, P_3, P_4, P_{a+1}\}$; The initial token value at P, $m_0=\{0,0, K_{jam}, q_{max}, m_{a,0}, m_{a+1,0}\}$. The 3 *transitions* have a meaning: input for t_1, output on t_3, and t_2 which govern traffic flow follows a non-linear pattern based on the TFD.

Tokens in the set *P* are denoted by the notation, $m=\{m_1, m_2, m_3, m_4, m_a, m_{a+1}\}$. Initial token $m_{a,0}$ must be greater than null to activate t_1, indicating the initial traffic flow $q_{a,0}$. If $m_{1,0}$ is null, means the initial condition for the

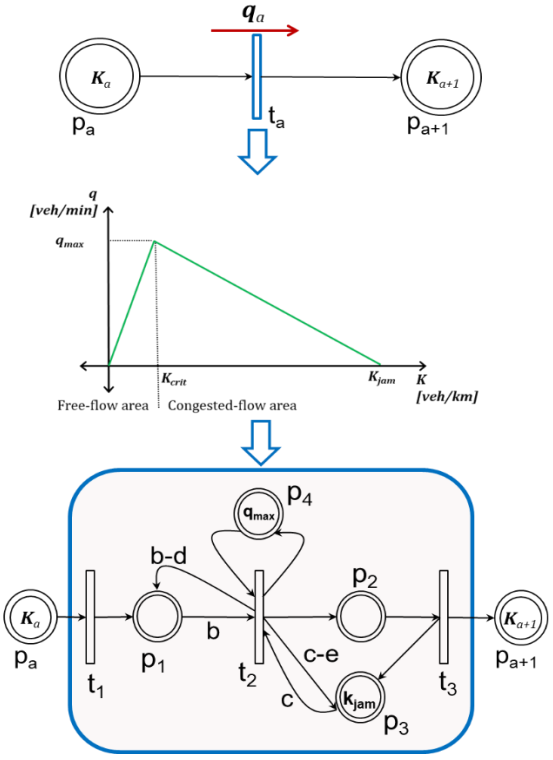

Figure 4. The HPN Continue Modelling of the TFD model

traffic flow in the TFD starts from null. The output of transition t_2 produces the actual output token for a single road section, with the resulting token stored in m_2. If $m_{2,0}$ is a null, it indicates that the vehicle density starts from an empty state. The internal firing speed parameter λ at each transition determines the final value of the transition current flow in steady state. t_1 and t_2 serve as reference transitions for transition t_3 , with their internal firing speeds $\lambda_{t_1}$and λ_{t_2} fixed at 1. The output from t_2 will activates the vehicle flow at the output of t_3. The internal firing speed parameter λ_{t_3} at the output of transition t_3 acts as a variable. Therefore, the internal firing speed λ_{t_3} determines the vehicle flow conditions at the end of the single road segment when steady state is reached, in accordance with the TFD. The initial token for $m_{3,0}$ is K_{jam}, representing the condition when a road section is completely congested. Finally, $m_{4,0}$ corresponds to q_{max}, indicating the maximum vehicle flow at a given moment. The result of the accumulated flow from t_3 is placed in p_{a+1} with tokens of m_{a+1}.

The basic mathematical model for the dynamics of the transition current flows f_1, f_2, and f_3 in this model, as shown in Figure 3, is represented by Equations 14-16, with $\lambda_{t_1} = \lambda_{t_2} = 1$ as reference values.

$$f_1 = \lambda_{t_1} \cdot m_a = m_a \tag{14}$$

$$f_2 = \lambda_{t_2} \cdot enab(t_2, \boldsymbol{m}) = \boldsymbol{min} \begin{cases} m_1/b \\ m_4 \\ m_3/c \end{cases} \tag{15}$$

$$f_3 = \lambda_{t_3} \cdot m_2 \tag{16}$$

The parameter λ_{t_3} for t_3 in free flow, equilibrium flow, and congested flow conditions is defined in Equation 17 below.

$$\lambda_{t_3} = \begin{cases} \frac{(q_{max} - m_a)}{m_2}, \text{when free} - \text{flow} \\ \frac{(q_{max} - m_a)}{K_{crit}}, \text{when equilibrium flow} \\ \frac{1}{c} \cdot \left(\frac{K_{jam}}{m_2} - 1\right), \text{when congested flow} \end{cases} \tag{17}$$

The input for this analysis method is the dynamic network structure of HPN Continue ($\mathcal{N}$, m_0). The structure of the single road section model with HPN Continue components, as shown in Figure 5, includes an incident matrix. This matrix is based on the following assumptions and is detailed in the Incident **Pre** and **Post**-Matrix shown in Figure 5. The **Pre** and **Post** matrix represent PN structure for an event model, showing the network configuration before and after an event occurs at a *transition*. The dynamics of the network structure in a PN model are determined by the token flow matrix, or incident matrix (C), which is calculated using the following Equation (7). The composition of the values from the **Pre** and **Post** incident matrices can be used to determine the slope of the vehicle flow diagram at the transition to the number of tokens for each preset transition. The values of the variables affecting the Incidence **Pre** and **Post**-Matrix are the weights on the arrows shown in Figure 5.

In the TFD model, the constant weight parameter determines the evolution of the token m_x within the value limits b, c, $(b - d)$, $(c - e) \in \mathbb{R}_{\geq 0}$. The weight parameter d determines the evolution of token m_1, while the weight parameter e determines the evolution of token m_3. In this study, the parameter values for the arrow is set to d = -1 and e = 1. The weight b and c are determined by the following Equations 18-19.

$$b = \frac{K_{crit}}{q_{max}} \tag{18}$$

$$c = -\frac{1}{V_{wave}} = \frac{(K_{crit} - K_{max})}{(q_{(K\max)} - q_{max})} \tag{19}$$

In the HPN Continue model, this function represents the flow of vehicles entering a road segment to form a TFD. The shape of the TFD is characterized by m_2 and f. The dynamics of token m_2, representing the number of vehicles at the exit point of the road section (output transition), rise from the initial value of m_2. Meanwhile, f represents the traffic flow of vehicles passing through the road segment. The number of vehicles (m_2) and traffic flow (f) are determined by the dynamics of the token flow $\dot{m}_1$, the relationship between m_1 and token flow $\dot{m}_2$, and the constraints on tokens m_2 and m_3. With a weight value of d = -1, the evolution of token m_2 increases until $m_2 + m_3 = K_{jam}$. The traffic flow is divided into free flow, represented by f_1, and congested flow, represented by f_3.

Under free flow conditions, the vehicle flow increases linearly in proportion to the vehicle density. The dynamics of token m_2, representing the number of vehicles at the exit point of the road section (output transition), rise from the initial value of m_2. This increase under free flow conditions continues up to the critical vehicle density limit (K_{crit}) and the maximum traffic flow (q_{max}). In free flow, the TFD forms as the token flow $\dot{m}_1$ increases from its initial value to the maximum flow $\dot{m}_1 = q_{max}$, with the maximum number of tokens $m_2 = K_{crit}$.

Pre	t_1	t_2	t_3
P_1	0	b	0
P_2	0	0	1
P_3	0	c	0
P_4	0	1	0
P_i	1	0	0
P_{i+1}	0	0	0

(a)

Post	t_1	t_2	t_3
P_1	0	b-d	0
P_2	0	0	1
P_3	0	c-e	0
P_4	0	1	0
P_i	1	0	0
P_{i+1}	0	0	0

(b)

Figure 5. Incidence Matrix (a) **Pre**, (b) **Post**

Consequently, the maximum value of $\dot{m}_1$ at steady flow boundary conditions, influenced by the synchronization of transition t_2, changes to equal $f_2 = q_{max}$. The parameter m_4 is constant and corresponds to the maximum vehicle flow (q_{max}).

Congested flow conditions arise when road segment usage m_2 depends on the available capacity of the road segment m_3, beyond the equilibrium flow boundary. The equation for determining λ_{t_3} under congested flow is based on the dynamics of token flow $\dot{m}_3$ and the linear invariance of flows m_2 and m_3. The weight c represents the constant operating mode during congested flow, defined by the wave speed (V_{wave}), and indicates the peak equilibrium flow point. This value captures the deceleration of token flow from output m_2 to input m_3. Congested flow occurs when vehicle flow exits at f_3 from transition t_3 within the range $q_{max} < f_3 < q_{Kjam}$. The accumulation of used vehicle space (m_2) and vehicle capacity limitations (m_3) leads to total congestion when the number of vehicles reaches the maximum capacity of the road segment (K_{jam}). The congested flow graph is determined by the number of vehicle tokens at place p_2, as m_2 serves as the **Pre**-incident matrix for transition t_3 from K_{crit} to K_{jam}.

4. DATA RETRIEVAL

Traffic flow data collection using a Virtual Loop Detector (VLD) was conducted at the Pasteur Gate on the Padaleunyi Highway. This location was selected because it serves as a major entry point for vehicles heading into Bandung, the third-largest city in Indonesia as seen Figure 6. VLD functions as a vehicle detection sensor on the highway road, estimating parameters such as the density, vehicle speed, and more (29, 30). Detectors are installed in two of the four lanes leading to the highway exit, while the other two lanes, which are in the opposite direction, are not monitored.

Currently, cameras are used as vehicle detectors, either to count the number of vehicles, vehicle speed, or detect collisions on the road (31). VLD works through a camera that activates a signal when a vehicle crosses a designated virtual area, activating a specific node (loop). From this virtual node, three key parameters are measured: the number of vehicles is determined by counting the frequency of active nodes in two zones of the same lane; vehicle speed is calculated by comparing the arrival times between zones in each lane with the actual distance between those zones; and the distance between vehicles is estimated from the time difference between active nodes within the same lane. The detector continuously collects real-time traffic flow data and sends it periodically to the central controller via short messages.



Figure 6. Data collection location for the study area: Pasteur Highway Gate

5. SIMULATION RESULT

5. 1. Macroscopic Modelling of Pasteur Highway

Traffic data from the Padaleunyi Toll Road to the Pasteur Toll Gate, downloaded from the server, is the most stable dataset. The data includes the following parameters: date, time, location ID, time span, number of vehicles, vehicle speed, and air temperature. The data was collected at 15-minute intervals over a one-month period. Figure 7 compares the flow-density relationship graph of the original data with the MFD model for traffic at the Pasteur highway gate. The minimum vehicle density recorded is 0.218 vehicles/km, corresponding to a traffic flow of 44 vehicles/hour passing through the Pasteur toll gate. On the other hand, the highest vehicle density reaches 82.256 vehicles/km, with a traffic flow of 3,208 vehicles/hour. The data shows a direct linear relationship between density and flow on average, indicating an increasing trend where the number of vehicles rises as traffic flow grows. However, some data points fall below this trend, affecting the variability in macroscopic model calculations and resulting in a downward trend.

5. 2. TFD modeling of Pasteur Highway

The timed HPN-ISS model, as shown in Figure 3, includes the

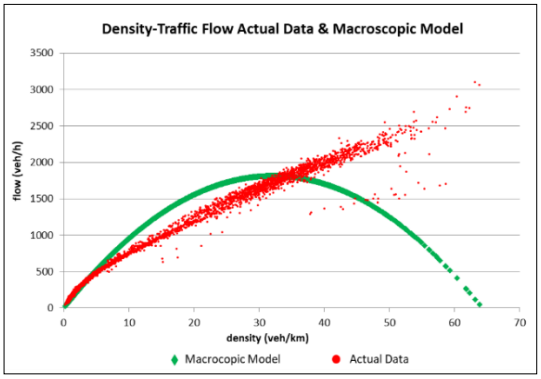

Figure 7. Comparison of density-traffic flow relationships between measurement data and MFD model approaches

dynamic structure parameters of the Petri net ($\mathcal{N}$, m_0) and the internal firing speed (λ) The macroscopic constant parameters that form the fundamental triangular diagram in the model are the average speed of multiple vehicles in free-flow and congested-flow conditions, the maximum vehicle flow (q_{max}), critical vehicle density (K_{crit}), and maximum vehicle density (K_{jam}) when the road section is fully congested. The final traffic conditions in the simulation are reflected in the vehicle flow and density at steady state, which can be determined through the internal firing speed parameter λ_{t_3} at the output transition t_3.

From the measurement data, an MFD is created using the Greenshield model method. This method involves forming a hyperbolic line trend based on the derivation of the equation for the linearity of the vehicle speed graph from the actual measurement data. The average difference across all data collection times is -0.703. Additionally, using the absolute percent error method, the average error value is -2.242%. Finally, a TFD model is created, requiring several parameters as summarized in Table 1.

The MFD model in Figure 7 can be simplified into a TFD representation. A complete analysis of the influencing variables in simulations using SimHPN includes is q_{max}, K_{crit}, K_{max}, $Q_{(Kmax)}$, and K_{jam}, as shown in Figure 8. The TFD model in Figure 8 is derived from the data in Table 1, focusing on the start point, peak point, and end point.

TABLE 1. TFD Model Forming Variables.

Variable		TFD Model	
		Per Hour	Per Minute
Start Poin	K_0	0.218 (veh/km)	0.218 (veh/km)
	q_0	24.48 (veh/h)	0.408 (veh/min)
Peak Point	K_{crit}	32.523 (veh/km)	32.523 (veh/km)
	q_{max}	1813.38 (veh/h)	30.223 (veh/min)
End Point	K_{jam}	63.833 (veh/km)	63.833 (veh/km)
	q_{jam}	47.64veh/h)	0.792 (veh/min)

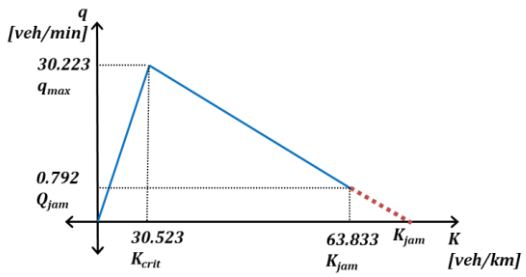

Figure 8. TFD model of the Pasteur highway

5. 3. HPN Continue Modeling of Pasteur Traffic Flow The value of the variables that form the matrix set in SimHPN according to the HPN Continue involves determining weights to create the Incident **Pre** and **Post**-Matrix. The formation of this simulated matrix will generate a diagram representing free flow and congested flow. Based on Table 1, the arrow weights are calculated according to Equations 18 and 19, resulting in b = 1.0761 km/min and c = 1.064 km/veh. The weight requirement for free flow is d = -1, while the weight for congested flow is e = 1. The Incidence **Pre** and **Post**-Matrix is then constructed as shown in Figure 9.

In addition to the Incident **Pre** and **Post**-matrices, several components of the HPN model are also required to form a TFD, consisting of: m_0 = [0;0;63.833;30.223;30.223;0]; λ = [1;1;30.223]; Type T = ['c';'c';'c']. Based on these variables, the HPN Continue model can be constructed, as shown in Figure 10.

Figure 10 of the PN model illustrates the number of vehicles, K_a, represented by tokens p_a, entering the Pasteur Gate Highway a road. The magnitude of traffic flow dynamics depends on the condition of the road segment represented by f_a. In the TFD-HPN Continue model (Figure 10), the recorded evolutionary changes at each shift in λ_t affect both the number of vehicles stored in m_2 and the traffic flow through the Pasteur Road section, represented by f_1 at t_1 and f_3 at t_3. The input variable that changes the parameter is the internal firing speed λ_{t_3} in the SimHPN, which reflects the dynamics of vehicle traffic flow changes to the Pasteur exit highway gate every minute. To establish free flow, the number of vehicles entering is continuously increased in m_2, from an initial value of q_0 = 0.408 to q_{max} = 30.223, while the flow of vehicles exiting the Pasteur toll gate under free-flow status is represented by f_1 at t_1. As the m_2 variable increases from q_{max} = 30.223 to q_{Kjam} = 63.833, based on the TFD-HPN Continue model (Figure 10), the flow transitions to represent congested conditions at the Pasteur toll gate, where the flow f_3 at t_3 shows a decreasing slope. This scenario in the TFD-HPN Continue model reflects congested flow.

Pre	t_1	t_2	t_3
P_1	0	1,076	0
P_2	0	0	1
P_3	0	1,064	0
P_4	0	1	0
P_i	1	0	0
P_{i+1}	0	0	0

(a)

Post	t_1	t_2	t_3
P_1	0	2,076	0
P_2	0	0	1
P_3	0	0,064	0
P_4	0	1	0
P_i	1	0	0
P_{i+1}	0	0	0

(b)

Figure 9. Incidence Matrix TFD-HPN Continue Model of the Pasteur Highway (a) **Pre**, (b) **Post**

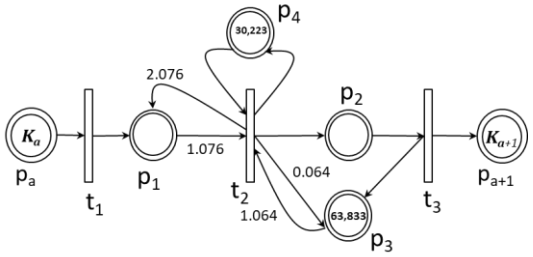

Figure 10. TFD-HPN Continue model for Pasteur traffic flow

5. 3. TFD-HPN Continue Model on the Pasteur Highway in SimHPN The equilibrium of each change in traffic flow through the Pasteur exit gate compared to the number of vehicles passing forms the TFD is shown in Figure 11. The simulation depicts the volume of vehicles flowing at the Pasteur gate, starting at 1 vehicle/min, with a value nearly equal to the road section's capacity of 0.93 vehicles/km. The traffic flow is directly proportional to vehicle density—the greater the traffic flow, the more vehicles pass through the toll road to the Pasteur gate. This situation is still considered free flow. When the number of vehicles reaches 31,914 vehicles/km, the flow peaks at 29,878 vehicles/min, indicating a shift from steady flow to congested flow. After reaching this stable flow, the traffic flow decreases inversely proportional to the number of vehicles on the Pasteur highway gate. In the SimHPN simulation, the maximum number of vehicles recorded is 63,755 vehicles/km, while the traffic flow passing through the Pasteur toll gate drops to 0.0739 vehicles/min.

Figure 12 provides a comparative illustration of a MFD model based on vehicle density-traffic flow measurement data at the Pasteur toll gate and a TFD using SimHPN. The differences between the two models are apparent. The TFD approach simplifies the system to expedite the process of traffic system supervision. In the MFD model, the diagram is divided into three segments:

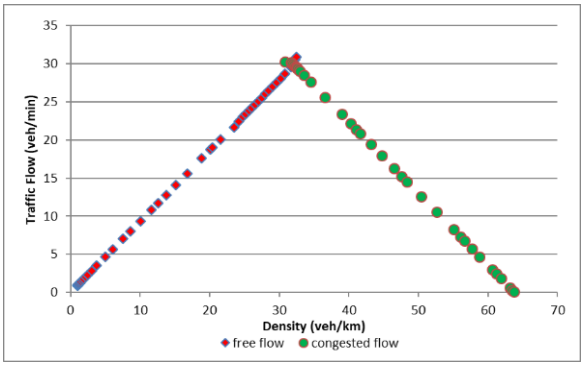

Figure 11. TFD-HPN Continue model for the Pasteur Highway

free flow, equilibrium flow, and congested flow. Conversely, the TFD approach only differentiates between two areas: free flow and congested flow, with boundaries defined by the maximum flow at the Pasteur toll gate. This division of traffic flow conditions results in the TFD having two distinct average speeds: the average speed during free flow, denoted as V_{free}, and the average speed during congested flow, referred to as V_{wave}. Three intersection points between the MFD model and the TFD-HPN Continue model are shown in Table 2.

Table 2 presents a comparison of vehicle density and traffic flow values between the MFD model and the TFD-HPN Continue model at three points. The comparison focuses on critical traffic flow-vehicle density conditions (q_{max}, K_{crit}) and saturated traffic flow-vehicle density conditions (Q_{jam}, K_{jam}). While there are slight differences in values, Table 2 and Figure 12 indicate that the TFD-HPN Continue model closely approximates the MFD model for the Pasteur highway.

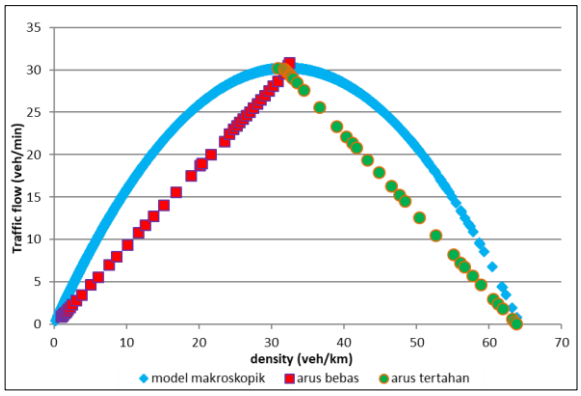

Figure 12. Comparison of traffic flow between the TFD-HPN Continue model and the MFD model

TABLE 2. Comparison of values between the MFD Model and the TFD-HPN Continue Model for the Pasteur Highway

Variable		MFD Model	TFD-HPN Model
Start Poin	K_0	0.218 (veh/km)	1 (veh/km)
	q_0	0.408 (veh/min)	0.93 (veh/min)
Peak Point	K_{crit}	32.523 (veh/km)	31.914 (veh/km)
	q_{max}	30.223 (veh/min)	29.999 (veh/min)
End Point	K_{jam}	63.833 (veh/km)	63.755 (veh/km)
	q_{jam}	0.794 (veh/min)	0.064 (veh/min)

6. CONCLUSION

This research aims to model the traffic flow-vehicle density relationship using TFD and HPN Continue, with

a focus on a single entrance ramp. TFD is chosen for its ability to simplify the model, expedite computational processes, and respond rapidly to dynamic changes in traffic flow and vehicle density. Data collected from the Pasteur highway road indicates that traffic flow tends to approach instability and is sensitive to changing conditions. After modeling with MFD using the Greenshield method, an HPN Continue approach is applied to the Pasteur highway road data to establish the TFD. The results demonstrate that TFD modeling with HPN Continue effectively represents the MFD of the Pasteur highway road. The simulation results showed that the differences between the TFD-HPN Continue model and the MFD model are as follows: K_{crit} by 1.87%, q_{max} by 0.74%, and K_{jam} by 0.12%.

Sensitivity analysis of the TFD-HPN Continue model has not yet been conducted to assess its response to parameter changes. This is recommended for future work to ensure reliability under real-world conditions. ML techniques, such as Random Forest and K-Nearest Neighbor (KNN), could improve data collection and analysis. Additionally, Long Short-Term Memory (LSTM) networks and Reinforcement Learning (RL) could predict vehicle flow and optimize toll gate traffic distribution.

Further development is essential to apply the TFD-HPN Continue model to multi-lane road networks and various designs, considering segment length and capacity. Challenges include modeling complex intersections without signals to analyze capacity evolution and queue dynamics, as well as optimizing traffic flow at signalized intersections with coordinated traffic lights. VISSIM or SUMO software can be used to validate the model with empirical data and simulate specific traffic scenarios.

7. REFERENCES

1. Suleiman G, Younes MK, Ergun M, Abushammala M, Aljaradin M. Highlighting Traffic Accidents on Roundabouts Using MRSS-AHP Expert System. Civil Engineering Journal. 2024;10(04). https://doi.org/10.28991/CEJ-2024-010-04-013
2. Ruangkanjanases A, Sivarak O, Weng Z-J, Khan A, Chen S-C. Using multilayer perceptron neural network to assess the critical factors of traffic accidents. HighTech and Innovation Journal. 2024;5(1):157-69. https://doi.org/10.28991/HIJ-2024-05-01-012
3. Sejdiu L, Tollazzi T, Shala F, Demolli H. Analysis of Traffic Safety Factors and Their Impact Using Machine Learning Algorithms. Civil Engineering Journal. 2024;10(9):2859-69. https://doi.org/10.28991/CEJ-2024-010-09-06
4. Ferrara A, Sacone S, Siri S, Ferrara A, Sacone S, Siri S. An overview of traffic control schemes for freeway systems. Freeway traffic modelling and control. 2018:193-234. https://doi.org/10.1007/978-3-319-75961-6_8
5. Hafram SM. Calibrating and validation microscopic traffic simulation models vissim for enhanced highway capacity planning. International Journal of Engineering, Transactions B: Applications. 2023;36(8):1509-19. https://doi.org/10.5829/ije.2023.36.08b.11
6. Tolba C, Lefebvre D, Thomas P, El Moudni A. Continuous and timed Petri nets for the macroscopic and microscopic traffic flow modelling. Simulation Modelling Practice and Theory. 2005;13(5):407-36. https://doi.org/10.1016/j.simpat.2005.01.001
7. Siri S, Pasquale C, Sacone S, Ferrara A. Freeway traffic control: A survey. Automatica. 2021;130:109655. https://doi.org/10.1016/j.automatica.2021.109655
8. Pasquale C, Sacone S, Siri S, Ferrara A. Traffic control for freeway networks with sustainability-related objectives: Review and future challenges. Annual Reviews in Control. 2019;48:312-24. https://doi.org/10.1016/j.arcontrol.2019.07.002
9. Harjono MS, Utomo DP. Pemodelan Ruas Jalan Tunggal dengan Diagram Fundamental Triangular equilibrium. Majalah Ilmiah Pengkajian Industri; Journal of Industrial Research and Innovation. 2019;13(2):93-102. https://doi.org/10.29122/mipi.v13i2.3472
10. Ferreira C, Neves LC. Macro modelling of traffic flow using continuous timed Petri nets. Transportation planning and technology. 2021;44(5):503-23. https://doi.org/10.1080/03081060.2021.1927304
11. Chuo HSE, Swa YH, Tan MK, Lim KG, Barukang L, Teo KTK, editors. Modelling Discrete Urban Traffic Network System with Cellular Automata. 2021 IEEE 19th Student Conference on Research and Development (SCOReD); 2021: IEEE.
12. Bouriachi F, Kechida S. Modelling and analysis of oversaturated intersections using jointly hybrid Petri net and hybrid automata. International journal of intelligent transportation systems research. 2018;16:138-50. https://doi.org/10.1007/s13177-017-0144-4
13. Mohammadi M, Dideban A, Moshiri B. A novel approach to modular control of highway and arterial networks using petri nets modeling. International Journal of Engineering, Transactions B: Applications. 2023;36:1578-88. https://doi.org/10.5829/ije.2023.36.08b.17
14. Díaz G, Macià H, Valero V, Boubeta-Puig J, Cuartero F. An Intelligent Transportation System to control air pollution and road traffic in cities integrating CEP and Colored Petri Nets. Neural Computing and Applications. 2020;32(2):405-26. https://doi.org/10.1007/s00521-018-3850-1
15. Ruan K, Li L, Chen Y, editors. Highway traffic modeling using probabilistic petri net models. 2020 IEEE 23rd International Conference on Intelligent Transportation Systems (ITSC); 2020: IEEE.
16. Zhang M, Abbas-Turki A, Lombard A, Koukam A, Jo K-H, editors. Autonomous vehicle with communicative driving for pedestrian crossing: Trajectory optimization. 2020 IEEE 23rd International Conference on Intelligent Transportation Systems (ITSC); 2020: IEEE.
17. Jafari S, Savla K, editors. On structural properties of optimal feedback control of traffic flow under the cell transmission model. 2019 American Control Conference (ACC); 2019: IEEE.
18. Guo Y. Dynamic-model-based switched proportional-integral state observer design and traffic density estimation for urban freeway. European Journal of Control. 2018;44:103-13. https://doi.org/10.1016/j.ejcon.2018.09.007
19. Kumbhar VB, Chavan MS, editors. A review of petri net tools and recommendations. International Conference on Applications of Machine Intelligence and Data Analytics (ICAMIDA 2022); 2023: Atlantis Press.
20. Khan ZH, Gulliver TA. A macroscopic traffic model based on transition velocities. Journal of computational science. 2020;43:101131. https://doi.org/10.1016/j.jocs.2020.101131

21. Sarkar NC, Bhaskar A, Zheng Z, Miska MP. Microscopic modelling of area-based heterogeneous traffic flow: Area selection and vehicle movement. Transportation Research Part C: Emerging Technologies. 2020;111:373-96. https://doi.org/10.1016/j.trc.2019.12.013
22. Aghamohammadi R, Laval JA. Dynamic traffic assignment using the macroscopic fundamental diagram: A review of vehicular and pedestrian flow models. Transportation Research Part B: Methodological. 2020;137:99-118. https://doi.org/10.1016/j.trb.2018.10.017
23. Daganzo CF, Geroliminis N. An analytical approximation for the macroscopic fundamental diagram of urban traffic. Transportation Research Part B: Methodological. 2008;42(9):771-81. https://doi.org/10.1016/j.trb.2008.06.008
24. Zhang L, Yuan Z, Yang L, Liu Z. Recent developments in traffic flow modeling using macroscopic fundamental diagram. Transport reviews. 2020;40(4):529-50. https://doi.org/10.1080/01441647.2020.1743918
25. Suwanno P, Kasemsri R, Duan K, Fukuda A. Application of macroscopic fundamental diagram under flooding situation to traffic management measures. Sustainability. 2021;13(20):11227. https://doi.org/10.3390/su132011227
26. Murata T. Petri nets: Properties, analysis and applications. Proceedings of the IEEE. 1989;77(4):541-80. https://doi.org/10.1109/5.24143
27. Signoret J-P, Leroy A, Signoret J-P, Leroy A. Petri Net Modelling. Reliability Assessment of Safety and Production Systems: Analysis, Modelling, Calculations and Case Studies. 2021:587-660. https://doi.org/10.1007/978-3-030-64708-7_33
28. Júlvez J, Mahulea C, Vázquez C-R. SimHPN: A MATLAB toolbox for simulation, analysis and design with hybrid Petri nets. Nonlinear Analysis: Hybrid Systems. 2012;6(2):806-17. https://doi.org/10.1016/j.nahs.2011.10.001
29. Po L, Rollo F, Bachechi C, Corni A, editors. From sensors data to urban traffic flow analysis. 2019 IEEE International Smart Cities Conference (ISC2); 2019: IEEE.
30. Harrou F, Zeroual A, Sun Y. Traffic congestion monitoring using an improved kNN strategy. Measurement. 2020;156:107534. https://doi.org/10.1016/j.measurement.2020.107534
31. Delavarian M, Marouzi O, Hassanpour H. A multilayer motion direction based model for tracking vehicles at intersections. International Journal of Engineering, Transactions A: Basics. 2020;33(10):1939–50. https://doi.org/10.5829/IJE.2020.33.10A.12

COPYRIGHTS

©2025 The author(s). This is an open access article distributed under the terms of the Creative Commons Attribution (CC BY 4.0), which permits unrestricted use, distribution, and reproduction in any medium, as long as the original authors and source are cited. No permission is required from the authors or the publishers.

Persian Abstract

چکیده

مقاله حاضر بر ایجاد یک مدل جریان ترافیکی ماکروسکوپی تمرکز دارد که پویایی‌های مهم ترافیک شامل تراکم و جریان ترافیک و سرعت متوسط را توصیف می‌کند. تغییرات در پویایی جریان ترافیک از طریق یک مدل ساده‌شده جریان ترافیکی ماکروسکوپی با شکل مثلثی ثبت می‌شود که به سیستم اجازه می‌دهد به سرعت به شرایط واقعی واکنش نشان دهد. مدل شکل مثلثی به نام نمودار بنیادی مثلثی (TFD) شناخته می‌شود که شرایط اساسی ترافیک شامل جریان آزاد، جریان تعادل و شرایط تراکم را نشان می‌دهد. این تحقیق از شبکه پتری هیبریدی (HPN) و شبیه‌ساز SimHPN برای توسعه مدل TFD استفاده می‌کند. پس از آن، مدل TFD-HPN به یک مطالعه موردی مربوط به ترافیک بزرگراه پاستور اعمال شد. این مقاله به‌طور موفقیت‌آمیزی یک مدل جریان ترافیکی ماکروسکوپی (TFD) را معرفی می‌کند و آن را با رویکرد شبیه‌سازی HPN ادامه می‌دهد. نتایج شبیه‌سازی نشان داد که تفاوت‌های بین مدل TFD-HPN و مدل نمودار بنیادی ماکروسکوپی (MFD) شامل K_{crit} با ۱.۸۷% و q_{max} با 0.74% و K_{jam} با ۰.۱۲٪ است. به‌طور خلاصه، مدل TFD-HPN توانایی خود را در شباهت به پویایی‌های ترافیک واقعی از طریق کاربرد آن در بزرگراه پاستور نشان می‌دهد.